

**MODELING EVOLUTION OF TSUNAMI AND ITS IMPACT
ON COASTAL VEGETATION**

TEH SU YEAN

UNIVERSITI SAINS MALAYSIA

2008

**MODELING EVOLUTION OF TSUNAMI AND ITS IMPACT
ON COASTAL VEGETATION**

by

TEH SU YEAN

**Thesis submitted in fulfillment of the
requirements for the degree
of Doctor of Philosophy**

February 2008

ACKNOWLEDGEMENTS

I am greatly indebted to Professor Koh Hock Lye for his supervision, stimulating suggestions and dedication that contribute significantly towards the completion of this thesis. Further, I would like to record my sincere appreciation to Associate Professor Ahmad Izani Md. Ismail for his constant encouragement and guidance as well as for the generous provision of facilities and space to complete this research. I spent a period of six months in the University of Miami in South Florida to conduct a significant part of this research (vegetation recovery) following a major pulse disturbance that would be induced by events such as a mega tsunami or a major hurricane. I take this opportunity to thank the Government of Japan, UNESCO and the UNESCO/Keizo Obuchi Research Fellowship for their generous financial support, which enabled me to achieve this goal. In particular, Professor Donald DeAngelis of University of Miami has been a pillar of inspiration and a source of useful insights, for whom I tender my sincere gratitude. Professor Leo Sternberg also from University of Miami has been a primary mover to initiate and sustain the research into the modeling of vegetation recovery induced by a competition between hardwood hammocks and mangroves, both of which are found in great abundance but with uneven distributions in southern Florida. This research on vegetation recovery model would not have been possible without the contributions from Professor Sternberg and Professor DeAngelis, to whom I am grateful. I was a recipient of a scholarship to participate in research activities in the International Center for Theoretical Physics (ICTP) located in Trieste, Italy, once in March and the second time in May 2007. I am indeed greatly indebted for the excellent academic atmosphere that is both inspiring and captivating. The School of Mathematical Sciences of Universiti Sains Malaysia together with the Institute of Graduate Studies have provided me on a continuous basis an ambience conducive to research. My parents have been a constant source of comfort during time of stress and

duress. I take this opportunity to record my deep gratitude. Finally, my friends, with whom I have wonderfully fond memory, have provided me with a stream of joys throughout the duration of my graduate study, without whom it would be almost unbearable to endure long and lonely nights.

TABLE OF CONTENTS

	Page
ACKNOWLEDGEMENTS	ii
TABLE OF CONTENTS	iv
LIST OF TABLES	viii
LIST OF FIGURES	ix
LIST OF SYMBOLS	xiv
LIST OF ABBREVIATION	xvii
ABSTRAK	xviii
ABSTRACT	xx
CHAPTER 1 : INTRODUCTION	1
1.1 Introduction to Tsunami	1
1.2 Tsunami Impacts and Hazards	2
1.3 Tsunami Resilient Community	5
1.4 Tsunami Modeling	6
1.5 Objectives of Thesis	7
1.6 Scope and Organization of Thesis	8
CHAPTER 2 : LITERATURE REVIEW	10
2.1 Introduction to Tsunami Impact Modeling	10
2.2 Source Generation Term	12
2.3 Shallow Water Equations	16
2.4 Numerical Models	22
2.5 Role of Mangrove	29
2.6 Mangrove Recovery	30
CHAPTER 3 : TSUNAMI PROPAGATION	33
3.1 Introduction	33
3.2 Shallow Water Equations	34
3.2.1 Analytical One-Dimensional Model	35
3.2.2 Analytical Two-Dimensional Model	36

3.3	Numerical Model TUNA-M2	37
3.3.1	Semi-Diurnal Tide	38
3.3.2	Tsunami in a Narrow and Long Reservoir	40
3.3.3	One-Dimensional TUNA-M1	42
3.4	Boundary Conditions	46
3.4.1	Reflective Boundary	46
3.4.2	Radiation Boundary	51
3.5	Initial Conditions	51
3.6	26 December 2004 Tsunami	54
3.6.1	Conceptual Analysis	54
3.6.2	Real Simulation	59
3.7	Tidal Records	65
3.8	Conclusion	67
CHAPTER 4 : TSUNAMI RUNUP		68
4.1	Introduction	68
4.2	Literature Review	69
4.2.1	Some Empirical Formulae	69
4.2.2	Semi-Analytical Method	73
4.3	NSWE for Runup	76
4.3.1	NSWE Model	77
4.3.2	Comparison between CRP and SRP	79
4.3.3	Comparison between RBCs	81
4.3.4	Test Results	82
4.3.5	Detail Wave Structure	87
4.4	Moving Boundary for Runup	89
4.5	Results and Discussion	92
4.6	Conclusion	94
CHAPTER 5 : ROLE OF MANGROVE		96
5.1	Introduction	96
5.2	Mangrove Drag Characteristics	97
5.2.1	Morison Equation	102
5.2.2	Drag Coefficient	102

5.3	Linear Approximation	105
	5.3.1 A Linear Example	107
	5.3.2 Sensitivity Analysis	108
5.4	Numerical Simulations	109
	5.4.1 Numerical Algorithm	109
	5.4.2 A Numerical Example	110
	5.4.3 Detail Wave Structure	113
	5.4.4 A Comparison	116
5.5	Sensitivity Analysis	118
	5.5.1 Wave Period vs. Forest Width	118
	5.5.2 Wave Period vs. Forest Density	122
	5.5.3 Forest Density vs. Forest Width	125
5.6	Malaysian Case Study	127
5.7	Conclusion	132
CHAPTER 6 : VEGETATION RECOVERY		133
6.1	Introduction	133
6.2	Mangrove-Hammock Feedback Model	135
6.3	The MANHAM Model	137
	6.3.1 Approaches	137
	6.3.2 Methodology	140
6.4	Model Simulations	146
6.5	Results and Discussion	148
	6.5.1 Impact of Seawater Inundation	158
	6.5.2 Thickness of Vadose Zone	158
6.6	Complex Hydrology	159
6.7	Potential Applications	166
6.8	Conclusion	166
CHAPTER 7 : CONCLUDING REMARKS		168
REFERENCES		171

LIST OF PUBLICATIONS	182
APPENDICES	
Appendix A TUNA-M2	184
Appendix B Snapshots of Runup	187
Appendix C Photos of Field Surveys	190
Appendix D Numerical Algorithm	194
Appendix E Runup Height Measurement	196

LIST OF TABLES

		Page
3.1	Simulated maximum elevations and arrival times, conceptual bathymetry	56
3.2	Simulated maximum elevations and arrival times, real bathymetry	58
3.3	Andaman tsunami source dimension obtained from literature	60
3.4	Maximum elevation (m) and arrival time (h) at the five observation points	61
3.5	Survey runup heights for the 26 December 2004 tsunami	64
4.1	Survey runup heights for the December 26 2004 tsunami	86
5.1	Parameter Values of drag characteristics	104
5.2	Decay number β (n,T) when $v_0 = 2$ m/s and $h = 2$ m	109
5.3	Half distance \hat{x} (n,T) when $v_0 = 2$ m/s and $h = 2$ m	109
5.4	Reduction ratio of elevation r_η	119
5.5	Reduction ratio of velocity r_u	119
5.6	Parameter values used to define the forest density	122
5.7	Reduction ratio of elevation r_η	123
5.8	Reduction ratio of velocity r_u	123
5.9	Reduction ratio of elevation r_η	125
5.10	Reduction ratio of velocity r_u	125
5.11	Measured parameter values of the Pantai Mas mangrove forest for three forest densities	128
5.12	Reduction ratio of elevation r_η of a 1000 m wide Pantai Mas forest	128
5.13	Reduction ratio of velocity r_u of a 1000 m wide Pantai Mas forest	128
5.14	Reduction ratio of elevation r_η of a 500 m wide Pantai Mas forest	130
5.15	Reduction ratio of velocity r_u of a 500 m wide Pantai Mas forest	130
6.1	Parameter values used in the simulations	145

LIST OF FIGURES

	Page
1.1 Countries affected by the recent 2004 Asian Tsunami	2
1.2 Boats and cars in Penang moved by the Andaman tsunami waves	4
1.3 Houses in Kuala Muda, Kedah destroyed by the Andaman tsunami waves	4
2.1 Geometry of the earthquake source	13
2.2 A solitary wave prescribed by Equation (2.1)	14
2.3 N-waves of (a) leading depression followed by an elevation (LDN) and (b) leading elevation followed by a depression (LEN)	15
3.1 Computational points for a staggered scheme	38
3.2 Analytical vs. TUNA-M2 for (a) elevation η , (b) velocity u and (c) velocity v	39
3.3 Tsunami propagation across a narrow, long and deep reservoir (a) initial velocity of -1 m/s for t from 0 to 700 s (b) zero initial velocity for t from 0 to 400 s	41
3.4 Propagation of waves with no dispersion, $\Delta t = 5$ s	45
3.5 Propagation of waves for an initial sinusoidal deformation	45
3.6 Propagation of waves with dispersion, $\Delta t = 2.5$ s	46
3.7 Tsunami propagation in a reservoir simulated by TUNA-M1 (a and b) and TUNA-M2 (c and d)	48
3.8 Tsunami propagation in a square with zero initial velocity (left to right) in 2D (a to f) and 3D (g to l) plots	49
3.9 Tsunami propagation in a square with simple radiation condition (left to right) in 2D (a to f) and 3D (g to l) plots	50
3.10 Tsunami propagation with initial velocity, $u = v = 1.0$ m/s	53
3.11 Tsunami propagation with initial velocity of 1.0 m/s in 4 different directions; (a) NW, (b) NE, (c) SE and (d) SW	53
3.12 Tsunami propagation from a line source, with velocity (a) 0 m/s, (b) 1 m/s due NE and (c) 14.14 m/s due NE	53
3.13 Study domain	55

3.14	Wave heights with initial velocities (a) 0.0 m/s and (b) 1.4 m/s for conceptual model	56
3.15	Wave heights with initial velocities (a) 0.0 m/s and (b) 1.4 m/s for actual simulations	57
3.16	The propagation of tsunami waves with initial velocity of 1.4 m/s for the conceptual model at intervals of 0.39 hour	58
3.17	Map of the study domain indicating the source (S) and observation points (A, B, C, D and E)	62
3.18	Elevation (m) at the five observation points due to a single source	62
3.19	Contour plots of the tsunami propagation towards Malaysia and Thailand at intervals of 10 minutes	63
3.20	Observed and predicted elevations at (a) Langkawi, (b) Lumut and (c) Butterworth	66
4.1	Sequence of solitary wave propagation (Equation 4.6)	71
4.2	FCTS scheme (CRP)	78
4.3	Staggered scheme (SRP)	78
4.4	CRP simulated η and u for semi-diurnal tide at (a) 12 (b) 36 and (c) 48-h	80
4.5	SRP simulated η and u for semi-diurnal tide at (a) 12 (b) 36 and (c) 48-h	81
4.6	(a) analytical solution, (b) TUNA RP simulated η and u by RBC3, (c) RBC2 and (d) RBC1	82
4.7	Comparison between using flux and velocity	84
4.8	Amplification of a soliton of wavelength $L=2700$ m across a domain of about 2000 m with slope=1.0	85
4.9	Tsunami wave runup onto beaches with concave slope	86
4.10	Bathymetry used in the simulation (not to scale)	88
4.11	Elevation η , velocity u and flux M at time (a) 0.125 (b) 0.175 (c) 0.225 and (d) 0.275 hour	88
4.12	Study domain (visually distorted due to scaling factor)	90
4.13	Snapshots of the wave runup onto a bottom slope of 0.05	93
4.14	Snapshots of the wave runup onto a dry land slope of 0.05	94

5.1	Dependence of A/V on the water depth for different mangrove species	99
5.2	Dependence of V_0/V on the water depth for different mangrove species	99
5.3	<i>Rhizophora stylosa</i> schematic diagram (top) actual photo (bottom)	100
5.4	<i>Bruguiera gymnorhiza</i> schematic diagram (top) actual photo (bottom)	101
5.5	Image of modeled unit mangrove tree	103
5.6	Wave transformation over the mangrove forest	108
5.7	Waveforms at interval of 0.05 hr with $n = 0.30$ at 12 to 13 km, denoting the presence of mangrove forest	112
5.8	Waveforms at 0.3 hr with $n=0.0$, 0.02 and $n=0.2 \text{ s/m}^{1/3}$	113
5.9	Waveforms at 0.3 hr with friction $n=0.02$ and without friction $n=0.0$ for Δx (a) 20.0 m (b) 10.0 m and (c) 5.0 m	114
5.10	Elevations η at $t=0.3$ hr for every halving of Δx , from 40.00 m to 1.25 m	115
5.11	Comparison between results using Manning friction term $n = 0.22$ (circle) and drag resistance term C_D (line) from 12 to 13 km	117
5.12	Reduction ratio of elevation r_η as a function of forest width W for a range of wave periods T	120
5.13	Reduction ratio of velocity r_u as a function of forest width W for a range of wave periods T	120
5.14	Dependence of reduction ratio of elevation r_η at location x (m) for wave period of 10 minutes	121
5.15	Dependence of reduction ratio of velocity r_u at location x (m) for wave period of 10 minutes	121
5.16	Reduction ratio of elevation r_η as a function of forest density for a range of wave periods T	124
5.17	Reduction ratio of velocity r_u as a function of forest density for a range of wave periods T	124
5.18	Reduction ratio of elevation r_η as a function of forest width for a range of forest density	126

5.19	Reduction ratio of velocity r_u as a function of forest width for a range of forest density	126
5.20	Location of Pantai Mas in Penang island	127
5.21	<i>Avicennia officinalis</i> in Pantai Mas mangrove forest	127
5.22	r_η of a 1000 m wide Pantai Mas forest as a function of forest density for a range of wave periods	129
5.23	r_u of a 1000 m wide Pantai Mas forest as a function of forest density for a range of wave periods	129
5.24	r_η of a 500 m wide Pantai Mas forest as a function of forest density for a range of wave periods	131
5.25	r_u of a 500 m wide Pantai Mas forest as a function of forest density for a range of wave periods	131
6.1	Hardwood hammock and mangrove transpiration and water uptake	138
6.2	Transpiration (mm day^{-1}) of mangrove vegetation and by freshwater hammocks as a function of vadose pore water salinity	142
6.3	Percentage of cells occupied by hammock and mangrove vs. salinity	146
6.4	(a) Topography used in the model simulation and (b) initial random distribution of hammocks (white) and mangroves (black) at the frequency of 0.85	147
6.5	Distribution of mangroves and hammocks (a) without a storm surge, and subject to (b) light (7.5 ppt), (c) medium (15 ppt) and (d) heavy (30 ppt) surges	149
6.6	Salinity in the vadose zone (a) without a storm surge, and subject to (b) light (7.5 ppt), (c) medium (15 ppt) and (d) heavy (30 ppt) surges	150
6.7	Snapshots of salinity (ppt) in the vadose zone at time intervals of 2.74 years during the heavy storm surge simulation (left to right and down)	152
6.8	Distribution of mangroves at time intervals of 2.74 years during the heavy storm surge simulation (left to right then down)	153
6.9	Fraction of cells occupied by hammocks as a function of the severity of the storm surge in terms of ppt saturation of the vadose zone	154

6.10	Average salinity (ppt) profiles along the elevation gradient for the scenario in which vegetation was artificially not allowed to change	155
6.11	Average salinity (ppt) profiles along the elevation gradient for the scenario in which vegetation was allowed to undergo successional changes	155
6.12	Elevational profiles showing the fractions of cells occupied predominately by hammocks vegetation for increasing vadose zone thickness with elevation	156
6.13	Elevation profile showing the fraction of cells occupied by hammocks for constant vadose zone thickness	156
6.14	Salinity (ppt) changes over time (day) in about (a) 0.2 m and (b) 1.0 m thick vadose zone (SS = storm surge)	157
6.15	Revision of Figure 6.1 to include a groundwater lens of variable salinity	160
6.16	Distribution of mangroves and hammocks (a) without a storm surge, and subject to (b) light (7.5 ppt), (c) medium (15 ppt) and (d) heavy (30 ppt) surges	162
6.17	Salinity in the groundwater lens (a) without a storm surge, and subject to (b) light (7.5 ppt), (c) medium (15 ppt) and (d) heavy (30 ppt) surges	163
6.18	Salinity in the vadose zone (a) without a storm surge, and subject to (b) light (7.5 ppt), (c) medium (15 ppt) and (d) heavy (30 ppt) surges	164
6.19	(a) Distribution of mangroves and hammocks, (b) salinity in the vadose zone and (c) salinity in the groundwater lens subject to a heavy storm surge	165
6.20	Percentage of cells occupied by hammocks at higher elevation areas vs. groundwater lens thickness, \hat{H} , subject to a heavy storm surge	165

LIST OF SYMBOLS

<i>Symbols</i>	<i>Descriptions</i>	<i>Units</i>
\hat{x}	half distance	m
\ddot{u}	water particle acceleration normal to the cylinder	m/s ²
\dot{u}	water particle acceleration normal to the cylinder	m/s ²
η	elevation	m
σ	wave frequency	s ⁻¹
γ	friction coefficient	dimensionless
β	decay number	m ⁻¹
ρ	water density	kg/m ³
ρ	porosity	dimensionless
η_0	Initial wave height	m
α_0	input of freshwater	mm/day
Δt	time step	s
$\Delta x, \Delta y$	spatial grid size	m
a	amplitude	m
A_0	projected area of trees under water surface, per 100 m ²	m ² /100 m ²
A_L	projection area of leaf part	m ² /100 m ²
A_R	projection area of root part	m ² /100 m ²
A_T	projection area of stem part	m ² /100 m ²
B_{Ai}	active tissue carbon of species i	g C m ⁻²
B_{Amaxi}	maximum value attainable by B_{Ai}	g C m ⁻²
B_{Ci}	carbon in plant biomass of species i	g C m ⁻²
b_{Ci}	leaf area per unit carbon	m ² / g C
c	wave celerity	ms ⁻¹
C_D	drag coefficient	dimensionless
C_{ij}	allometric parameters governing the amount of energy allocated to active tissue (leaves)	dimensionless
C_M	inertia coefficient	dimensionless
D	total depth	m
D_f	diameter of obstacles member	m
D_L	diameter of leaf part	m
D_R	diameter of each prop root	m
D_T	diameter of stem	m
E	evaporation	mm/day

F	wave force per unit length on a circular obstacles	N/m
F_{dry}	fraction of water allocated to each dry cell	dimensionless
f_{Ci}	measures of canopy dominance of species i	dimensionless
g	gravity	ms^{-2}
h	depth	m
H	offshore wave height	m
\hat{H}	depth of groundwater lens	mm
H_L	diameter of leaf part	m
H_R	diameter of each root part	m
H_T	diameter of stem part	m
I	surface gradient	dimensionless
I	solar irradiance	$\text{GJ m}^{-2} \text{d}^{-1}$
I_{NF}	Infiltration rate	mm/day
k	wave number	m^{-1}
k_l	light extinction factor	dimensionless
ℓ	study domain size	m
L	wave length	m
L_{Cvi}	litterfall of species i	$\text{g Cm}^{-2} \text{day}^{-1}$
l_{Ai}	active tissue litter loss rate	yr^{-1}
l_{Wi}	woody tissue litter loss rate	yr^{-1}
M	flux in the x-direction	$\text{m}^2 \text{s}^{-1}$
N	flux in the y-direction	$\text{m}^2 \text{s}^{-1}$
M_F	wave momentum flux	$\text{m}^2 \text{s}^{-1}$
M_{Cvi}	respiration of species i	$\text{g Cm}^{-2} \text{day}^{-1}$
m_{Ai}	active tissue respiration rate	yr^{-1}
m_{Wi}	woody tissue respiration rate	yr^{-1}
n	manning coefficient	$\text{sm}^{-1/3}$
N_R	number of prop roots per tree	dimensionless
N_T	number of trees per 100 m^2	dimensionless
P	precipitation	mm/day
P_L	leaf porosity	dimensionless
Q_i	effect of salinity on productivity of species i	$\text{mmd}^{-1}/\text{mmd}^{-1}$
R	runup height	m
r_{η}	reduction ratio of elevation	m/m
R_1	hardwood hammock uptake of water	mm/day
R_2	mangrove uptake of water	mm/day
R_f	linear friction coefficient	s^{-1}

R_{TOTAL}	plant uptake of water	mm/day
r_u	reduction ratio of velocity	m/m
S_0	salinity of ocean water	ppt
S_{Ci}	leaf index area of species i	m^2/m^2
S_V	salinity of the pore water in the vadose zone	ppt
S_{wt}	salinity of the underlying saline groundwater	ppt
t	time	s
T	wave period	s
u	velocity in the x-direction	ms^{-1}
u_0	Initial velocity	ms^{-1}
U_{Cvi}	gross productivity of species i	$g\ Cm^{-2}day^{-1}$
v	velocity in the y-direction	ms^{-1}
V	control volume	m^3
V_0	total volume of trees/obstacles under water	m^3
v_0	maximum velocity	ms^{-1}
V_L	volume of leaf part	m^3
V_M	total volume of obstacles	m^3
V_R	volume of root part	m^3
V_T	volume of stem part	m^3
W	forest width	m
w_{Ci}	light competition coefficient of species i	dimensionless
x	distance	m
z	depth of the vadose zone	mm

LIST OF ABBREVIATION

ADI	Alternating Direction Implicit
ATWC	Alaska Tsunami Warning Center
COULWAVE	Cornell University Long and Intermediate Wave Modeling Package
FTCS	Forward in Time Central in Space
FUNWAVE	Fully nonlinear Boussinesq Water Wave Model
GEBCO	General Bathymetric Chart of the Oceans
IOC	Intergovernmental Oceanographic Commission
JPS	Jabatan Pengairan dan Saliran
LDN	Leading Depression N-wave
LEN	Leading Elevation N-wave
MBC	Moving Boundary Condition
MOST	Method of Splitting Tsunami
MSL	Mean Seal Level
NOAA	National Oceanic and Atmospheric Administration
NSWE	Nonlinear shallow water equation
NTHMP	National Tsunami Hazard Mitigation Program
PNG	Papua New Guinea
PTWC	Pacific Tsunami Warning Center
RBC	Radiation Boundary Condition
SMF	Submarine Mass Failure
SWE	Shallow Water Equations
TIME	Tsunami Inundation Mapping Effort
TOPICS	Tsunami Open and Progressive Initial Condition System
TUNAMI-N2	Tohoku University's Numerical Analysis Model for Investigation of Near Field Tsunamis
UNESCO	United Nations Educational, Scientific and Cultural Organization
WC/ATWC	West Coast and Alaska Tsunami Warning Center

PEMODELAN EVOLUSI TSUNAMI DAN IMPAKNYA TERHADAP TUMBUHAN PERSISIRAN PANTAI

ABSTRAK

Fokus utama tesis ini ialah pemodelan pergerakan gelombang tsunami merentasi laut sejurus selepas gempa bumi dan evolusi gelombang tersebut apabila menghampiri persisiran pantai. Objektif utama kajian ini ialah untuk menghasilkan kebolehan di kalangan komuniti saintifik Malaysia untuk menghasilkan peta banjir dan evakuasi yang berguna untuk mitigasi impak tsunami. Kerjasama antara ahli sains dan komuniti tempatan untuk mengurangkan impak negatif tsunami melalui pendidikan dan komunikasi berkesan amat diperlukan dalam mewujudkan komuniti yang mampu menahan impak tsunami. Pelbagai model simulasi tsunami yang berdasarkan persamaan air cetek diperkenalkan untuk memberi asas kepada pembangunan model simulasi tsunami bernama TUNA. TUNA-M2 digunakan untuk simulasi pergerakan gelombang tsunami merentasi laut dalam, berikutan tsunami Andaman yang berlaku pada 26 Disember 2004. Ketinggian paras gelombang tsunami tersebut pada persisiran pantai di Pulau Pinang dan kawasan barat laut Malaysia disimulasi dengan menggunakan model TUNA-RP di mana ketinggian gelombang yang disimulasi oleh model TUNA-M2 digunakan sebagai input. Pengalaman dan pemerhatian di seluruh dunia menandakan keberkesanan peranan pokok bakau dalam pengurangan ketinggian gelombang. Simulasi model menandakan bahawa ketinggian gelombang sebanyak 3 m yang biasa sepanjang persisiran pantai di Pulau Pinang semasa tsunami Andaman boleh dikurangkan sehingga 1 m dengan kehadiran pokok bakau yang mempunyai ciri-ciri tertentu. Ini menunjukkan bahawa kawasan persisiran pantai di Pulau Pinang yang mungkin ditimpa gelombang setinggi 3 ke 4 m boleh dikatakan selamat dengan kehadiran pokok bakau yang mempunyai litupan yang bagus. Maka, perlindungan pokok bakau yang sedia ada dan pemulihan pokok bakau yang telah diganggu oleh tsunami merupakan suatu komponen yang penting dan perlu dalam

aktiviti yang menyumbang kepada pengwujudan komuniti yang mampu menahan impak tsunami. Pemodelan pemulihan tumbuhan berikutan suatu pembersihan yang mungkin disebabkan oleh tsunami mega atau taufan besar dapat memberi kefahaman untuk mencapai pemulihan berkesan pokok bakau yang diganggu atau dimusnahkan oleh suatu tsunami besar. Kefahaman yang diperolehi daripada kajian pemulihan tumbuhan di selatan Florida berguna untuk aplikasi pemulihan dan penanaman semula pokok bakau di Malaysia pada masa hadapan.

MODELING EVOLUTION OF TSUNAMI AND ITS IMPACT ON COASTAL VEGETATION

ABSTRACT

The main focus of this thesis is the modeling of earthquake-induced tsunami propagation across the deep ocean and their subsequent runup along the coastal beaches. The primary objective of this research is to develop the capability within Malaysia scientific communities to produce inundation and evacuation maps that will be useful for mitigating the impacts of tsunamis. The collaboration between scientists and local communities, via effective education and communication, to mitigate the adverse impacts of tsunami is crucial towards the development of tsunami resilient communities. Various tsunami simulation models based upon the shallow water equations are introduced, to provide the basis for the development of an in-house tsunami simulation model TUNA. TUNA-M2 is used to simulate tsunami propagation across the deep ocean following the 26 December 2004 Andaman tsunami. The tsunami runup wave heights along beaches in Penang and northwest Malaysia are then simulated by runup model TUNA-RP, using propagation wave heights simulated by propagation model TUNA-M2 as input. Experiences and observations worldwide indicate the positive role of mangroves in reducing wave heights. Model simulations indicate that a wave height of 3 m, which are common along Penang beaches during the Andaman tsunami, could be reduced to around 1 m with the presence of mangroves of certain desirable characteristics. This would imply that beaches in Penang with potential wave heights of 3 to 4 m might be rendered safe in the presence of good mangroves coverage. Hence, preservation of existing mangrove forests and recovery of mangroves disturbed by tsunami is an integral component of activities contributing towards tsunami resilient communities. Modeling vegetative recovery following a major pulse inundation, as would be induced by a mega tsunami or a major hurricane, would provide insights for achieving efficient recovery of mangroves

disturbed or destroyed by a major tsunami. The insights gained from this research on vegetation recovery conducted in South Florida would be useful for future application for mangrove recovery and replanting in Malaysia.

CHAPTER 1

INTRODUCTION

1.1 Introduction to Tsunami

Tsunamis are ocean waves that can be generated by an abrupt displacement of large volumes of water in the ocean caused by an earthquake, submarine landslide, volcanic eruption, meteorite impact, or by human activities such as nuclear explosions in the deep ocean. A typical tsunami comprises a series of waves of long periods and long wavelengths, generated by impulsive vertical disturbances of the sea floor in a body of deep water, typically more than 1000 m deep. A tsunami is formed when the seafloor is suddenly raised or lowered due to a violent earthquake. The most destructive tsunamis are formed from the occurrence of large earthquakes, with an epicenter or fault line located near or on the deep ocean floor. These usually occur in regions of the earth characterized by high seismic activities due to the collision of two plates along tectonic boundaries. A tsunami may also be caused by a violent horizontal displacement of water, as in the case of a submarine landslide in the ocean or large lake. All oceanic regions of the earth are subjected to the threat of tsunami; however, tsunamis are more concentrated in the Pacific Ocean and its marginal seas, popularly known as the *Ring of Fire*. A tsunami is basically a series of waves that originate from deep ocean water, traveling with very high speeds, and long periods and wavelengths. But as the wave travels towards the shallow shore, their wavelengths are progressively reduced, while the wave heights will usually increase accordingly. The tsunami that devastated the shorelines of eleven countries fringing the Indian Ocean on 26 December 2004 (Figure 1.1) was triggered by a mega-thrust earthquake with a large magnitude of 9.3 on the Richter scale, making it one of the most powerful in the past 100 years. A volume of water amounting to 200 trillion tons (or 200 trillion m³) was displaced 10 m vertically in a split second. The initial wave heights at the epicenter

were around 10 m, but increased progressively to exceed 30 m as they arrived at Banda Aceh beaches. Mega-thrust earthquakes are potentially very destructive and are created when one tectonic plate in the Earth's crust slip under another, as in the case of the Andaman earthquake on 26 December 2004. Another mega earthquake-tsunami combination took place on 28 December 1908, when a 7.2 magnitude quake struck Messina, Italy, killing an estimated 100,000 inhabitants. A 7.8 magnitude earthquake near Alaska generated a destructive tsunami in 1946 causing extensive damage to the neighboring Hawaiian Islands, with wave heights exceeding 35 m.

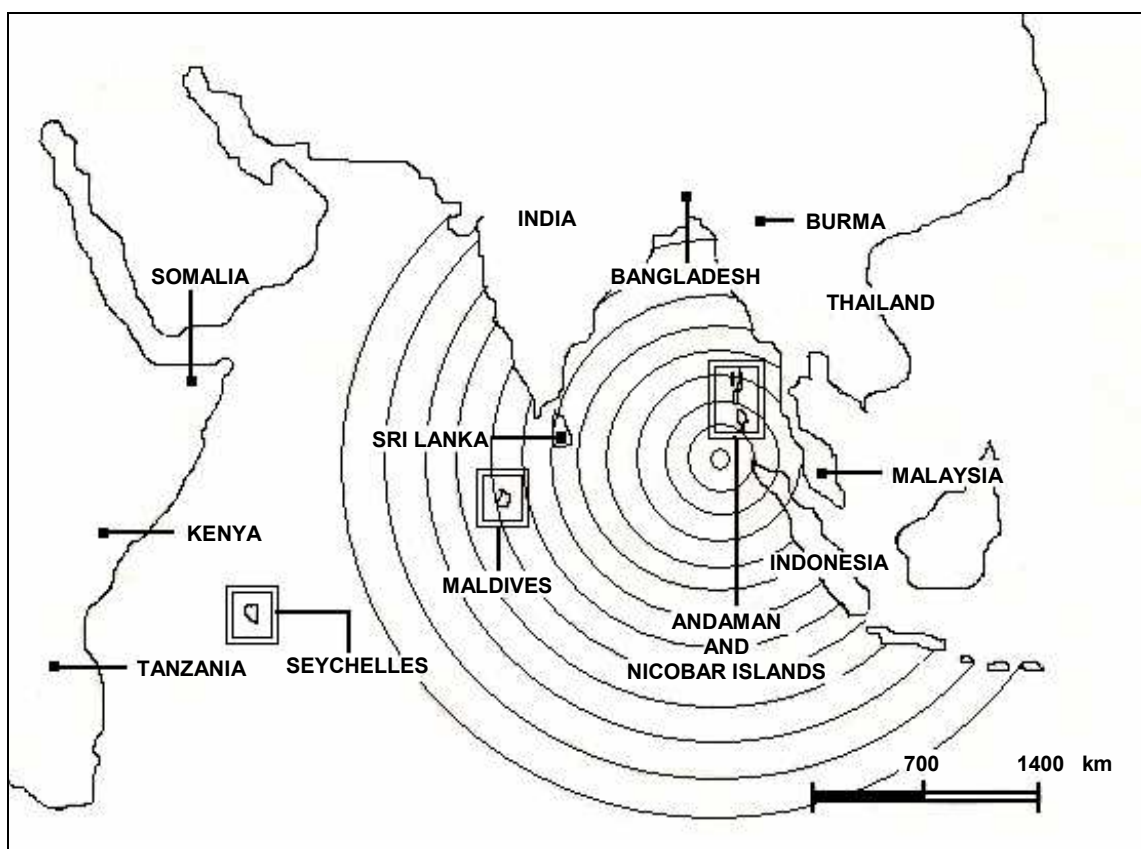


Figure 1.1: Countries affected by the recent 2004 Asian Tsunami

1.2 Tsunami Impacts and Hazards

The Andaman tsunami that occurred on 26 December 2004 has caused tremendous damage to properties and the loss of around 250, 000 lives along the affected coastal regions, particularly in the Province of Aceh, Indonesia. Previously perceived as safe from tsunami hazards, Penang and parts of northwest Malaysia were

not spared the agony created by that tsunami. The waves that arrived at the beaches in Penang exceeded 3 m at some places, with forces great enough to move boats and cars (Figure 1.2), while along the coasts of Kedah, many homes were destroyed (Figure 1.3). A total of 68 persons were killed in Malaysia, with 32 occurring in Penang alone. There is ample scientific evidence that suggests that tsunamis of such magnitudes will likely occur again in the region, due to the built up of stresses caused by the subduction of tectonic plates. Because of these potential hazards of future tsunamis, several efforts have been initiated to develop early warning systems and other tsunami mitigation measures to be put in place in these affected regions, which will be linked to the global tsunami early warning network to mitigate the adverse impacts of tsunamis (Morrissey, 2005). The capability to predict the characteristics of tsunami propagation and runup, notably wave heights, inundation distances and times of arrival, is essential in this early warning system. This capability will also be useful in the development of coastal zone management best practices that appropriately incorporate tsunami mitigation concepts and regulations. As tsunamis typically travel with high speeds exceeding 360 km/hour or 100 m/s in the deep ocean, early warning systems may not be able to provide adequate time for affected coastal regions to take protective mitigation measures, if the epicenter is close to the affected coasts. Hence coastal zone management practices that incorporate measures that could mitigate tsunami impacts are critically essential.

This thesis will therefore focus on modeling the impacts of tsunamis, with particular reference to the 26 December 2004 tsunami, with the assistance of a set of in-house tsunami numerical simulation models TUNA, developed in this thesis for this purpose. The role of mangroves in reducing wave heights and wave speeds will be modeled to provide the capability to assess the effectiveness of mangroves in tsunami mitigation. Much of mangroves in the affected areas in Malaysia were destroyed by the Andaman tsunami, giving rise to a concern over the potential adverse impacts should a

tsunami occur at a place where mangroves were destroyed. Hence the recovery and rehabilitation of mangroves is considered an integral part of tsunami mitigation measures. However, recent efforts to replant mangroves in Malaysia have met with little success. To provide scientific input towards successful recovery of mangroves after mega-pulse destruction and seawater inundation, this thesis will develop a model to simulate mangrove recovery after a mega pulse inundation following a large tsunami. This modeling was performed for the coastal region in south Florida, as data needed for this modeling analysis are available there. The pulse inundation of saline water is caused by mega storm surges induced by large hurricanes, but the effects are the same as though it was created by a tsunami. It is hoped that this modeling analysis would be extended to Malaysian mangroves when data are available.



Figure 1.2: Boats and cars in Penang moved by the Andaman tsunami waves



Figure 1.3: Houses in Kuala Muda, Kedah destroyed by the Andaman tsunami waves

1.3 Tsunami Resilient Community

Since the Andaman tsunami in 2004, several tsunamis of lesser scale but with significant impacts have occurred. There are scientific indications that significant earthquakes and tsunamis may continue to pose great risks and hazards to these coastal regions. Hence, developing community disaster management and risk mitigation capability is essential to protect coastal communities and to mitigate the impacts when a tsunami occurs in the near future. The concept and practice of developing tsunami resilient communities has been successful in reducing tsunami impacts in many nations including Japan and the Hawaiian islands. Numerical simulations of tsunami risks for the purpose of the establishment of mitigation measures are an integral component of the development of the capability of community disaster management. Inundation maps and evacuation maps that are useful to provide critical information to tsunami resilient communities can be developed from these tsunami simulations. These maps provide useful scientific documents and supporting evidence for tsunami resilient communities to develop risk management strategies and to devise effective mitigation measures. Expertise is presently available from research and operational centers catering to tsunami resilience and mitigation, such as the Pacific Tsunami Warning Center (PTWC) located in Hawaii, established soon after the 1946 Alaska tsunami that killed 173 people in Hawaii. Following the 1964 Alaska tsunami, the Alaska Tsunami Warning Center (ATWC) was formed in Palmer, Alaska, which was subsequently renamed the West Coast and Alaska Tsunami Warning Center (WC/ATWC), upon the formation of the US National Tsunami Hazard Mitigation Program (US NTHMP) in 1997. The US NTHMP defines tsunami resilient communities as having the following characteristics (Bernard, 2005):

- a. Understanding the nature of the tsunami hazards;
- b. Having the tools to mitigate the hazards;
- c. Disseminating information about tsunami hazards;

- d. Exchanging information with other at-risk areas;
- e. Institutionalizing planning for tsunami disaster.

The fundamental basis for tsunami mitigation planning consists of the following steps: Identify hazard zones, develop inundation maps, disseminate evacuation maps; turn vague concerns and abstract issues into clarified and concrete action plans; and implement the plan during a tsunami event. To achieve these goals the following infrastructure components are needed: Adequate seismic network, robust numerical models, sufficient deep-sea bed pressure sensors (tsunameters), dense coastal tide gages, and an effective Education and Community Awareness Program. The ultimate objective is to enable the coastal communities to evacuate the tsunami risk zones in a timely and orderly manner with minimal disruptions, and to provide guidance for subsequent search and rescue operations. For this purpose, the coastal community needs credible and reliable evacuation route maps and the means to receive and confirm correct tsunami warnings, which can be achieved in part by numerical modeling.

1.4 Tsunami Modeling

The Tsunami Inundation Mapping Effort (TIME) Center was thus established in the USA to develop an infrastructure to support tsunami inundation modeling to enable the development of evacuation mapping effort. Thus far, a total of 22 modeling efforts were completed by 2005 for 113 local communities serving 1.2 million people in USA. In conjunction with the Method of Splitting Tsunami (MOST), these inundation models have evolved to become the fundamental tsunami hazard assessment tools (González et al., 2005); for example, to issue tsunami warnings in addition to tsunami inundation mapping. Nevertheless, it is extremely difficult to issue correct tsunami warnings. Out of 20 tsunami warnings issued in Hawaii since 1946, 15 were false alarms, mainly

because coastal amplification factors vary significantly and because seismic data often translate to tsunami data imprecisely. It is hoped that tsunami modeling will help to reduce errors in early warnings issued. While correct tsunami warnings can save lives, false alarms are expensive and embarrassing. Tsunami warning and inundation modeling is a science that is rather imprecise. While it is generally accepted that an earthquake of magnitude 7 and above on the Richter scale may be capable of triggering a life-threatening tsunami, a smaller 5.2 earthquake in 1930 generated a tsunami of 6 m in California, a wave height far above what is deemed safe (below 3 m). In view of these often unreliable estimates of tsunami waves characteristics, education becomes the primary tool for tsunami mitigation, in which the following are deemed essential: Recognize the physical signs of impending tsunami; understand what areas are at risk; know when and how to evacuate, regardless of the predictions. In short, tsunami modeling should be integrated with other holistic approaches to achieve the goals of tsunami resilient communities.

1.5 Objectives of Thesis

The objectives of this thesis are as follows:

1. To develop tsunami simulation models TUNA-M2 and TUNA-RP;
2. To implement tsunami propagation model TUNA-M2 for the purpose of simulating tsunami wave heights offshore at depths of about 50 m;
3. To implement TUNA-RP for the purpose of generating tsunami wave runup heights along beaches of Penang and northwest Malaysia;
4. To assess by means of TUNA-RP the role of mangroves towards tsunami mitigation;
5. To develop and implement mangrove recovery model to assist in rehabilitation of mangroves destroyed by seawater inundation.

1.6 Scope and Organization of Thesis

This thesis will begin in Chapter 1 with an introduction to tsunami and its hazards, drawing insights from the experience of the Andaman tsunami and other tsunamis that occurred in the past. The need for developing tsunami resilient communities is then explored, which leads to the realization of the contributions of tsunami modeling towards achieving this goal, which is the primary focus of this thesis. The objectives, scope and organization of this thesis are then described.

Chapter 2 will provide a review of related literature, beginning with an introduction to tsunami modeling, based upon the commonly used shallow water equations. Some existing tsunami models are discussed and their merits briefly touched on, with the aim of motivating the development of an in-house tsunami model TUNA developed in this thesis. This is followed by a brief exploration of models to simulate vegetation recovery and competition after a major pulse disturbance, as would be induced by a mega tsunami or storm surge caused by a high impact hurricane.

A brief introduction to tsunami propagation model sets the tone for Chapter 3, which is devoted to the development and implementation of TUNA-M2 (Appendix A), used to simulate tsunami propagation from a source to an offshore depth of about 50 m. The importance of appropriate boundary conditions and initial conditions is highlighted, with particular reference to the Andaman tsunami and its impacts on Penang and northwest Malaysia, to which the remaining part of Chapter 3 is devoted. Deliberation regarding the usefulness of tidal records in Malaysia will round up this chapter.

The modeling of the runup of tsunami waves as they enter shallow coastal regions and beaches will be discussed in Chapter 4, which will introduce several

empirical formulae abstracted from the literature. This will lead to TUNA-RP, the model developed in this thesis for simulating tsunami runup along the shallow beaches. The response of tsunami runup to various conceptual beach slopes and shapes will be simulated to provide useful insights (Appendix B). This chapter will end with a summary of tsunami runup heights along beaches of Penang and parts of northwest Malaysia, using a method that incorporates moving boundaries, to provide guidelines for coastal zone management.

Significant parts of Malaysian coastal regions are fringed by mangrove forests, which are known to play some role in reducing the adverse impacts of tsunami. Chapter 5 will present the simulation of the role of mangroves in tsunami mitigation, in which a typical mangrove is represented schematically in such a manner to facilitate its incorporation into the model framework of TUNA-RP. Field measurements of mangrove trees were also conducted to obtain the parameters needed for the simulation (Appendix C). It will be shown that mangroves of certain characteristics may effectively reduce the impact of a tsunami to a safe level for Penang.

Large tracks of mangroves may be destroyed by mega tsunamis. The recovery of these disturbed mangroves is the focus of Chapter 6. A vegetation recovery model is proposed and developed for application to the recovery of forests covered with both hardwood hammocks and mangroves in southern Florida, chosen as a study site because of the rich data available for calibration and analysis. A major pulse inundation, as would be caused by either a tsunami or by hurricane-induced storm surges, is chosen as the initial salinity conditions for this analysis. Further refinement of this model for application to Malaysian mangroves is proposed for future research, to be performed when the required data are available. Chapter 7 will provide a short exposition to recommendations for further research to conclude this thesis. Finally, further details are deferred to the Appendices.

CHAPTER 2

LITERATURE REVIEW

2.1 Introduction to Tsunami Impact Modeling

Tsunami is a rare event that may inflict severe loss and pain to coastal communities living in the impacted regions. The Andaman tsunami that occurred in 2004 is an event with an estimated return period or recurrence interval of 500 to 1000 years, meaning it occurs once every 500 to 1000 years. However, there are ample scientific evidences to suggest that a tsunami of similar level of destruction may not be ruled out for this region in the near future. Hence the need to develop tsunami resilient communities is beyond any reasonable doubts.

A tsunami begins with an abrupt displacement of massive volume of water triggered usually by seismic activities. The displaced water column then radiates outwards, thus creating a tsunami that travel with high speeds and with potentially high waves. These waves can travel long distances, for example, the tsunami generated by an earthquake in Chile in 1960 crossed the Pacific Ocean and struck the Japanese coastlines after one day. However, most tsunamis that caused damage are generated by sources located at short distances of less than 300 km, known as near-field tsunamis. When the waves reach the shallow coastal areas, they slow down; heighten in water elevations and velocities and subsequently break along the beaches, creating an environment that can be highly dangerous to life and properties. This part of tsunami evolution creates dispersion of the waves, giving rise to waves with different frequencies or spectrum and different propagation speeds. Because of the difficulty in modeling this complicated flow regimes near shore, some models would simulate propagation up to 10 to 30 m contour and use the wave heights at this depth to infer maximum runup. Tsunami inundation maps for Hawaii up until the late 1990s have

been developed by this simple technique. However, field surveys of the 1992-1996 tsunamis showed that this approach produced predictions that differed by a factor of three to ten compared to field observations. Subsequent models hence would include a component that simulates the runup process by various techniques, with most using ad hoc and heuristic arguments for flow over dry land, for example, the assumption of hydrostatic pressure locally at the toe of the runup. This runup simulation is performed by essentially 1D models, for their simplicity and efficiency, superimposed onto 2D models of propagation, as is utilized in MOST model (Titov, 1997). This approach will also be used in this thesis. These runup models typically predict an amplification factor ranging between 2 to 6, strongly suggesting under prediction of runup heights simulated by models without a runup component.

The destructive strength of the tsunami begins with the initial waves generated at the source, known as the source generation or initial condition. The subsequent propagation in the deep ocean may be described by the so-called mildly nonlinear shallow water equations (NSWE) that may be solved by either analytical solutions or numerical codes such as MOST, TUNAMI-N2 and TUNA. More sophisticated numerical codes that include high nonlinearity and dispersivity are also available, such as GEOWAVE, which is based upon the Boussinesq approximations. Fully nonlinear potential flow theory has been used by Grilli and Svendsen (1989) and Titov (1997) to reproduce details of breaking wave fronts, details that are not reproduced by SWE models. However, the overall wave behavior of concern such as amplitudes and runup heights remains essentially unchanged. Due to the immense computational cost, this potential flow theory remains unpopular. Similarly, the full Navier-Stokes equations are not used to model long-wave runup.

Tsunamis generated by abrupt vertical uplifts of water column are better understood than those caused by submarine landslides. Near-field tsunamis generated

by submarine landslides can be potentially more dangerous than one created by uplift of similar volume, particularly in deep water. A simple reason is that the slide depth, of the order of hundreds or even thousands of meters, may be high in deep water, as compared with uplift, which is capped by the uplift of the sea floor that rarely exceeds 10 m. The potential energy associated with submarine landslides can therefore be much higher and more focused than that created by uplift of similar volume. Hence, near-field tsunamis triggered by submarine landslides can be devastating.

Recent observations and analysis suggest that coastal vegetations, such as mangroves, play an important role in mitigating the impacts of tsunamis, if the tsunami wave heights do not exceed 3 to 4 m. To quantify the relationship between mangrove properties and wave reductions, simulation models have been developed to assess the role of mangroves (Teh et al., 2007a). Tsunamis can destroy vast tracks of coastal mangrove forest. The subsequent species succession process may be analyzed by careful and thorough laboratory experiments and field surveys in conjunction with model simulations (Sternberg et al., 2007; Teh et al., 2008). Understanding how coastal ecosystems respond to perturbations, either abrupt or continuous, is important for proper coastal management in order to optimize coastal resources utilization, minimize losses of valued ecosystems and maximize available management options. Knowledge gained from this analysis can be helpful in the recovery and rehabilitation of mangrove forests destroyed by tsunamis.

2.2 Source Generation Term

An earthquake occurring near the seabed produces a co-seismic deformation that can trigger a perturbation of the sea floor, leading to a tsunami. This co-seismic deformation is normally much more rapid (one order of magnitude faster) than the characteristic time involved in the tsunami wave propagation. Further, the length scale

of this sea floor deformation is normally much larger than the water depth. These characteristics will produce an initial sea surface deformation that is presumed to be equal to the co-seismic vertical displacement of the sea floor (Okada, 1985). This surface deformation forms the initialization of the tsunami wave generation, sometimes called the *initial conditions*. Typically less than 1 % of the total energy released by the earthquake is transferred to tsunami initial waves, rendering the conversion of seismic parameters into tsunami characteristics imprecise. Hence, various estimations of initial condition for the 2004 Andaman tsunami have appeared in the literature. Some model simulations have even resorted to utilizing source initial condition as a calibration parameter (Titov, 1997). For tsunamis generated by submarine landslides or failures, the initial waveforms at the source are more difficult to derive. The wavelengths are shorter, implying increase significance of wave dispersion in subsequent propagation. Only co-seismic source generation is considered in this thesis, since the focus is on the Andaman tsunami, which is generated by co-seismic vertical surface deformation. The slow and often inaccurate estimations of earthquake source parameters (Figure 2.1) remain an obstacle to on time tsunami predictions.

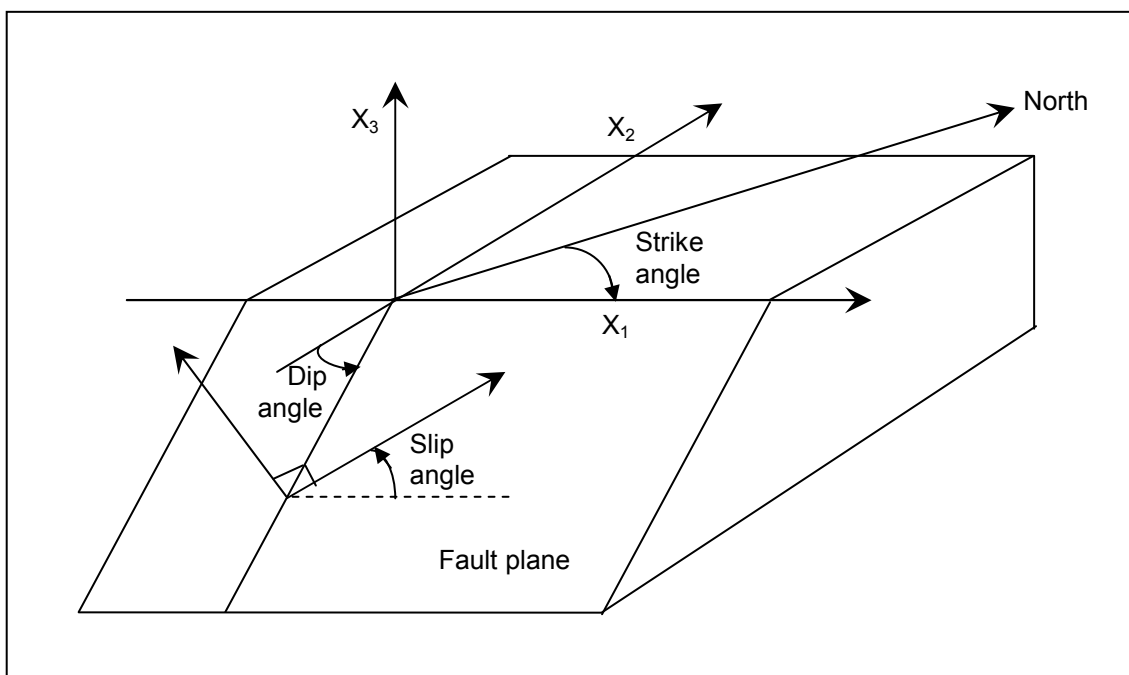


Figure 2.1: Geometry of the earthquake source

Waveforms: Sinusoidal, Solitary, N-waves

As of now three waveforms are commonly used in tsunami theoretical models and numerical simulations. The simplest is the sinusoidal wave of the form $\sin(\sigma t - kx)$, which is the solution of simple tide or tsunami model. The term $(\sigma t - kx)$ signifies a traveling wave that preserves its waveform as it travels forward. In much the same way, the waveform $e^{-(\sigma t - kx)}$ is a traveling wave that preserves its form for all time t . In a more general way any function of the form $f(\sigma t - kx)$ represents a traveling wave, with a speed of σ/k .

A second waveform is the solitary wave. A solitary wave that enters a region at the location x_1 when $t = 0$ is defined as (2.1) below (in dimensionless term).

$$\eta(x,0) = \frac{H}{h} \operatorname{sech}^2 \left(\sqrt{\frac{3H}{4h}} (x - x_1) \right) \quad (2.1)$$

A solitary wave as shown in Figure 2.2 appears to look like a half sine curve, and may be conceived as such for convenience.

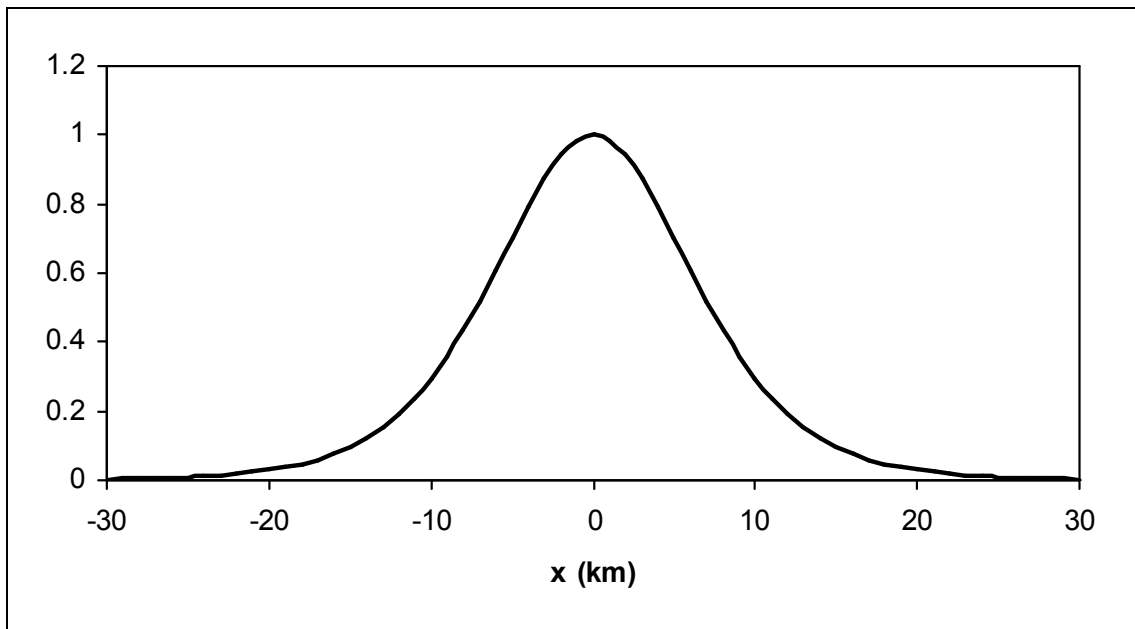


Figure 2.2: A solitary wave prescribed by Equation (2.1)

Recent observations of tsunami waves, however, indicate the existence of a series of waves with either a leading depression followed by an elevation or a leading elevation followed by a depression (Tadepalli and Synolakis, 1994; Smith, 2005). This type of wave is called an N-wave, with the first form being referred to as a Leading Depression N-wave or LDN, while the second is known as Leading Elevation N-wave or LEN (Figure 2.3). However, a wave with one single hump is sometimes used for its simplicity. This would not give rise to misinterpretation if the intention were merely to predict maximum wave heights and not the actual sequence of the time series. A tsunami may in fact be thought of as a series of N-waves.

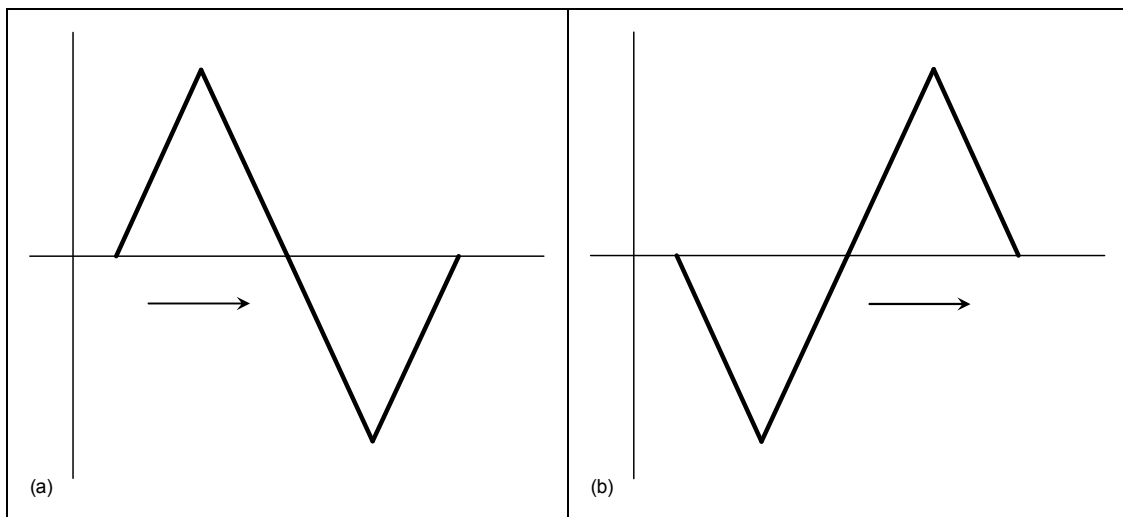


Figure 2.3: N-waves of (a) leading depression followed by an elevation (LDN) and (b) leading elevation followed by a depression (LEN)

Gaussian Hump

To generate the initial surface disturbance that will produce the wave propagation, a single hump of the Gaussian form $\eta = a e^{-(x/b)^2}$ has been successfully used by several authors, where a and b are arbitrary constants chosen to fit the initial wave (Yoon, 2002). This Gaussian hump simulates the initial rise in water level due to the sudden upward movement of the seabed, caused by an earthquake. With these simple initial conditions for a coseismic tsunami, then the analytical solution of the

simplified 1D tsunami is $\eta = a e^{-((x-ct)/b)^2}$, where $c = \sqrt{gh}$ is the wave velocity. The progressive waves propagate forwards in the positive x-direction. This type of Gaussian hump initial conditions will be used in some of the simulations performed in this thesis, in part because of its simplicity, and in part because this initial waveform appears to work well for tsunami generated by co-seismic vertical displacement. This certainly is true if the objective is to reproduce maximum wave heights, and not the fine details of subsequent waveforms.

2.3 Shallow Water Equations

Since tsunami wavelengths (tens or hundreds of km) are much larger than the ocean depths (km), and their amplitudes (m) are much smaller than the water depths (km), tsunamis are considered as *shallow water wave (SW)*, following the long wave (small amplitude) theory. In the shallow water theory, valid for a small amplitude and non dispersive propagation, the wave velocity (*celerity*) c is given by $c = \sqrt{gh}$, where g is the gravity acceleration and h is the sea depth (Ippen, 1966). For a depth h of 1000 m, for example, the wave velocity is 100 m/s (360 km/hour), assuming g is rounded up to 10 m/s^2 . This means that this tsunami will travel a distance of 100 m in one second, or a distance of 360 km in an hour. When the tsunami approaches the coast, the water depth h decreases and the wave velocity c slows down. For example at 10 m depth, c is only 10 m/s. While the periods (T) remain constant, the wavelengths (L) decrease, following the relationship $L \sim \sqrt{gh}$. The conservation of energy in the smaller volume of water (because of decreasing depths) produces nonlinear waves with heightened amplitudes and increased currents. The shallow water model (long wave theory) can still be applied to the tsunami as long as the wavelengths remain much larger than the water depths, and the water depths remain much larger than the amplitudes (Hérbert et al., 2005).

Under these assumptions, the hydrodynamic Navier-Stokes equations describing the conservation of mass and momentum can be depth averaged, leading to the following shallow water equations (SWE),

$$\frac{\partial(\eta+h)}{\partial t} + \nabla[u(\eta+h)] = 0 \quad (2.2)$$

$$\frac{\partial(u)}{\partial t} + (u\nabla)u = -g\nabla\eta + \Sigma f \quad (2.3)$$

where h is the sea depth and η is the water elevation above mean sea level, u is the depth-averaged horizontal velocity vector, g is the gravity acceleration and f represents bottom friction and Coriolis forces.

Polar Coordinates

For distant or far-field tsunami modeling (1000 km to 10000 km), the waves propagate over a long distance, then the curvature of the earth may be important. In this situation the SWE may be best represented in the polar form as follows (Nagano et al., 1991; Titov et al., 2005b),

$$\frac{\partial M}{\partial t} + \frac{gh}{R_e \cos \theta} \frac{\partial \eta}{\partial \varphi} = fN, \quad \frac{\partial N}{\partial t} + \frac{gh}{R_e} \frac{\partial \eta}{\partial \theta} = -fM, \quad (2.4)$$

$$\frac{\partial \eta}{\partial t} + \frac{1}{R_e \cos \theta} \left[\frac{\partial M}{\partial \varphi} + \frac{\partial}{\partial \theta} (N \cos \theta) \right] = 0 \quad (2.5)$$

where θ and φ are latitude and longitude, R_e is the radius of the Earth, $f = 2\omega_e \sin \theta$ is the Coriolis parameter, ω_e is the Earth rotation frequency, M and N are discharge fluxes along the latitude and longitude, $h(x,y)$ is unperturbed water depth.

Cartesian Coordinates

For near-field tsunami modeling (up to 1000 km), the shallow water equations in Cartesian Coordinates as follows should be used (IOC, 1997; Zahibo et al., 2006).

$$\frac{\partial \eta}{\partial t} + \frac{\partial M}{\partial x} + \frac{\partial N}{\partial y} = 0$$

$$\frac{\partial M}{\partial t} + \frac{\partial}{\partial x} \left(\frac{M^2}{D} \right) + \frac{\partial}{\partial y} \left(\frac{MN}{D} \right) + gD \frac{\partial \eta}{\partial x} + \frac{gn^2}{D^{7/3}} M \sqrt{M^2 + N^2} = 0$$

$$\frac{\partial N}{\partial t} + \frac{\partial}{\partial x} \left(\frac{MN}{D} \right) + \frac{\partial}{\partial y} \left(\frac{N^2}{D} \right) + gD \frac{\partial \eta}{\partial y} + \frac{gn^2}{D^{7/3}} N \sqrt{M^2 + N^2} = 0$$

Here, discharge fluxes (M, N) in the x- and y- directions are related to velocities u and v by $M = u(h+\eta) = uD$, $N = v(h+\eta) = vD$. The shallow water equations can be solved by several methods, such as the finite element methods used in Koh (1988) for the Penang Channel. The evolution of earthquake generated tsunami waves has three distinct stages: generation, propagation and runup. Analytical models have been used in many situations to represent a tsunami for each phase of the tsunami evolution.

Analytical Model

While analytical models cannot describe the details of land-sea geometry nor of the topographic complexities of ocean basins, they help in clarifying the physical nature of the processes involved, and in the interpretation and selection of laboratory models used to validate the numerical models. Analytical models are also useful for elementary sensitivity studies and in outlining the basic nature of the phenomena, providing valuable insights and understanding. The SWE may be simplified to the following linear equations in 1D as follows.

$$\frac{\partial \eta}{\partial t} = -h \frac{\partial u}{\partial x}, \quad x \in (0, \ell), \quad t \geq 0 \quad (2.6)$$

$$\frac{\partial u}{\partial t} = -g \frac{\partial \eta}{\partial x}, \quad x \in (0, \ell), \quad t \geq 0 \quad (2.7)$$

This may be reduced to the wave equation

$$\eta_{tt} = c^2 \eta_{xx} \quad (2.8)$$

where $c = \sqrt{gh}$ is the wave celerity or group velocity. The general solution of (2.8) is given by $f(x-ct)$ for any differentiable function f . In particular, $\sin(x-ct)$ and $e^{-(x-ct)}$ are typical solutions used.

Fourier-Laplace Transform

In one form of the analytical solutions, Fourier-Laplace Transform has been used to solve the shallow water equations. Haugen et al. (2005) applies analytical models based upon and extending the work by Watts (2001) by means of Fourier transform. A linear shallow water solution for the tsunami generation and propagation has been obtained by the Fourier-Laplace Transform (Trifunac et al., 2003) defined for some function $f(x, y, t)$ by

$$\bar{f}(\vec{k}; s) = \int_{-\infty}^{\infty} e^{-ik_2y} \left[\int_{-\infty}^{\infty} e^{-ik_1x} \left[\int_0^{\infty} e^{-st} f(x, y, t) dt \right] dx \right] dy$$

In the transform space, the water elevation $\eta(x, y, t)$ is given by

$$\bar{\eta}(\vec{k}; s) = \frac{s^2 \bar{\zeta}(\vec{k}; s)}{s^2 + \omega^2} \frac{1}{\cosh(kh)}$$

where $\bar{\zeta}(\vec{k}; s)$ is the transform of the motion of the ocean bottom, and

$$\omega = gk \tanh(kh)$$

is the circular frequency of the wave motion, k is the wave number, and g is the acceleration due to gravity. The long wavelength tsunami velocity (celerity) is given by $c = \sqrt{gh}$. Finally inverse Fourier transform is performed on $\bar{\eta}(\vec{k}; s)$ by Fast Fourier Transform to obtain $\eta(x, y, t)$ as follows.

$$\eta(x, y, t) = \frac{1}{2\pi} \int_{-\infty}^{\infty} e^{-ik_2y} \left[\frac{1}{2\pi} \int_{-\infty}^{\infty} e^{-ik_1x} \bar{\eta}(\vec{k}; t) dk_1 \right] dk_2$$

The long wavelength limit of $\bar{\eta}(\vec{k}; s)$ is $\lim_{k \rightarrow 0} \bar{\eta}(\vec{k}; t) = 0$.

The analytical approach, based upon NSWE, by means of Laplace-Fourier Integral was used by Liu et al. (2003) to model forced long waves on a sloping beach. Since the model is based upon the NSWE, the analytical solution is only accurate for small slopes.

Runup and Inundation

While most models used for propagation are based upon the SWE, runup modeling needs to consider nonlinearity induced by varying depths and possibly dispersive wave properties. Recently, many researchers have observed that the neglect of nonlinearity for runup simulation usually results in an underestimation of the predicted maximum wave height. A simple nonlinear SWE is used by many for its simplicity as follows.

$$\frac{\partial \eta}{\partial t} + \frac{\partial(u(\eta+h))}{\partial x} = 0 \quad (2.9)$$

$$\frac{\partial u}{\partial t} + u \frac{\partial u}{\partial x} + g \frac{\partial \eta}{\partial x} = 0 \quad (2.10)$$

Numerical instability of the solution occasionally appears in the form of sawtooth oscillations of the free surface. This is not surprising since a singularity is anticipated at the intersection of the free surface and the rigid boundary (Maiti and Sen, 1999). A moving boundary technique is often used to investigate wave runup and rundown with depth-averaged equations. Small grid sizes are used to ensure that wet-dry boundary location travels a significant numbers of grid points (greater than 10) during runup or rundown. To reduce the computational instabilities at the wet-dry interface, some researchers added bottom friction and eddy viscosity into the momentum equation. Highly nonlinear and weakly dispersive equations, if they are used, are solved using a high order finite difference scheme. Highly nonlinear Boussinesq-type equation models are sometimes used (Lynett et al., 2002).

COULWAVE

Zelt (1991) used a Lagrangian form of the Boussinesq type equation to simulate shoreline movement. This model produced maximum runup that compared well with experimental value but the shape of the wave as it traveled up the slope did not compare as favorably. A new moving boundary treatment for wave propagation was proposed by Lynett et al. (2002) using depth-integrated equations, where linear interpolation near the wet-dry boundary is utilized. The model used is nicknamed COULWAVE, for Cornell University Long and Intermediate Wave Modeling Package. The moving boundary technique is numerical-stable and does not require any additional dissipative mechanisms. It has been applied to both 1D and 2D problems. Small grid size is sometimes used mainly to make certain that the boundary location travels a significant number of grid points (>10) during runup and rundown. Comparisons indicate a significant improvement over weakly nonlinear Boussinesq equation results of Zelt (1991) and the nonlinear shallow water results of Titov and Synolakis (1995). The model has also been validated using long wave resonance in a parabolic basin and runup on a conical island.

For surging wave, on plane and impermeable slopes, Hunt (1959) recommended the simple runup formula as a simple rule of thumb guide,

$$R/H \approx 3.0 \quad (2.11)$$

where R is the maximum vertical runup from SWE and H is wave height (assumed to be the deep water wave height).

Solitary Wave Runup

Runup of solitary wave on impermeable plane slope have been studied, giving rise to both empirical and theoretical formulations for maximum runup as well as numerical simulation models for the entire runup sequence (Li and Raichlen, 2001; 2003; Carrier et al., 2003). Most of these formulations are derived from laboratory

experiments. It remains an open question whether these approaches are applicable to tsunami runup process. A theoretical runup equation for non-breaking solitary wave was developed by Li and Raichlen (2001) as follows.

$$\left(\frac{R}{h}\right)_{Li} = 2.831(\cot \alpha)^{1/2} \left(\frac{H}{h}\right)^{5/4} + 0.293(\cot \alpha)^{3/2} \left(\frac{H}{h}\right)^{9/4} \quad (2.12)$$

Here R is the runup height, H and h are the wave height and water depth at the toe of the incline slope just before the runup respectively, and α is the slope angle. This equation well fits the experimental data of Hall and Watts (1953) and Synolakis (1986; 1987) for slopes with $\cot \alpha = 1.0, 2.08, 2.14$ and 3.73 .

Relative wave runup has also been shown to be directly proportional to the maximum depth integrated wave momentum flux M_F as follows (Hughes, 2004).

$$\frac{R}{h} = 1.82 (\cot \alpha)^{1/5} \left(\frac{M_F}{\rho g h^2}\right) \quad (2.13)$$

2.4 Numerical Models

To overcome the shortcoming inherent in analytical solutions, numerical solutions may be used. There are several numerical models to simulate some or all phases of tsunamis. The MOST (Method of Splitting Tsunami) numerical model, based upon the shallow water equations, computes all three stages, and provides a complete tsunami simulation evolution. The MOST model is closely associated with the activities of the Tsunami Inundation Mapping Efforts (TIME). Another model commonly used is TUNAMI-N2, developed by Imamura of Tohoku University. There are also other models available. For example, GEOWAVE is a comprehensive tsunami simulation model, formed in part by combining the Tsunami Open and Progressive Initial Condition System (TOPICS) with the fully nonlinear Boussinesq water wave model (FUNWAVE).

GEOWAVE has been reported to accurately simulate tsunami runup and inundation in cases where other codes have failed (Watts et al., 2003).

MOST

The MOST model is based upon the SWE (2.2) to (2.3). The solution technique used is the explicit finite difference method on leap-frog staggered grids. This is achieved by splitting the governing equations for momentum into a pair of two equations, each containing only one space variable. This method of splitting saves computational memory and time, in much the same manner as is achieved in the Alternating Direction Implicit (ADI) method. The two systems of equations can then be solved sequentially at each time step by using explicit finite difference scheme. The explicit methods have proven to be efficient for this type of SWE. The MOST model has been extensively tested against various laboratory experiments (Titov and Synolakis, 1998) and verified by successfully reproducing field data for many historical tsunamis (Titov and Gonzalez, 2001; Titov et al., 2005a, b). Details of the MOST model applications for tsunami inundation mapping projects are available in Titov et al. (2003). The MOST model is designed with several nested computational grids for high-resolution inundation simulation. Three levels of computational grids are normally used to properly simulate three phases of computation: tsunami generation in deeper ocean, wave propagation through the ocean and inundation at impacted shallow coastal areas. To reproduce correct wave dynamics during the inundation computation, high-resolution grids are used. This high-resolution computation requires high quality bathymetry and topography data. MOST does not include bottom friction term in its formulation, contrary to normal practices used in other models, for example in TUNAMI-N2. There are several reasons for not using the friction term in MOST, foremost of which is the fact that friction term is not important in deep ocean and that it is very difficult to determine the friction coefficients a priori. Calculation of the inundation evolution over the dry bed involves moving boundary conditions, in which

the shoreline algorithm uses a time dependent space step $\Delta x(t)$. Additional grid points are introduced or removed as needed during the computation. During runup, additional grid points are introduced to accommodate more wet points; while during rundown the numbers of wet grid points are reduced sequentially in an analogous manner when the wet grids become dry. The MOST model has been used successfully to reproduce field measurements from the 1993 Hokkaido-Nansei-Oki tsunami at Okushiri Island, Japan (Titov and Synolakis, 1997). The model is reportedly able to predict even extreme runup value of 30 m for that event.

TUNAMI-N2

The numerical model, TUNAMI-N2 was originally created by Professor Fumihiko Imamura of the Disaster Control Research Center of the Tohoku University through the Tsunami Inundation Modeling Exchange (TIME) Program (Goto et al., 1997). TUNAMI-N2 is one of the common tools used for studying the propagation and coastal runup and inundation of tsunami waves. The solution technique is in principle similar to that used in the MOST model, except it includes the friction term. It has also been used to investigate the mode of free oscillations of coastal basins with general geometry and bathymetry, in addition to tsunami simulation. TUNAMI-N2 has been used to model tsunami wave field dynamics for the Java Sea where earthquakes generated large tsunami waves several times (Zahibo et al., 2006). The bathymetry for the Java Sea is taken from GEBCO (British Oceanographic Data Center) with mesh grid of 1 km. Boundary conditions on the land correspond to the full reflection (vertical wall approximation) and on the open boundary, free passage of the wave is imposed. The tsunami source is modeled by an ellipsoidal with semi axis 60 km by 20 km and the wave heights of 1 or 5 m. With friction term ignored, the results of the numerical simulations correspond to the theoretical prediction very well. In the deep ocean, friction is small due to the large depth and can be ignored without causing significant discrepancy between the simulation results and theoretical prediction.